HHS Public Access

Author manuscript

J Inorg Biochem. Author manuscript; available in PMC 2016 September 01.

Published in final edited form as:

J Inorg Biochem. 2015 September ; 150: 182–188. doi:10.1016/j.jinorgbio.2015.03.010.

Caged oligonucleotides for studying biological systems

Brittani K. Ruble, **Sean B. Yeldell**, and **Ivan J. Dmochowski***

Department of Chemistry, University of Pennsylvania, 231 S. 34thStreet, Philadelphia, PA 19104

Abstract

Light-activated ("caged") compounds have been widely employed for studying biological processes with high spatial and temporal control. In the past decade, several new approaches for caging the structure and function of DNA and RNA oligonucleotides have been developed. This review focuses on caged oligonucleotides that incorporate site-specifically one or two photocleavable linkers, whose photolysis yields oligonucleotides with dramatic structural and functional changes. This technique has been employed by our laboratory and others to photoregulate gene expression in cells and living organisms, typically using near UV-activated organic chromophores. To improve capabilities for *in vivo* studies, we harnessed the rich inorganic photochemistry of ruthenium bipyridyl complexes to synthesize Ru-caged morpholino antisense oligonucleotides that remain inactive in zebrafish embryos until uncaged with visible light. Expanding into new caged oligonucleotide applications, our lab has developed Transcriptome *In Vivo* Analysis (TIVA) technology, which provides the first noninvasive, unbiased method for isolating mRNA from single neurons in brain tissues. TIVA-isolated mRNA can be amplified and then analyzed using next-generation sequencing (RNA-seq).

1. Introduction

Photochemistry is essential to life on Earth, as most organisms depend on photochemical processes for their existence. Well-studied photo-biochemical reactions include photosynthesis [1], DNA damage [2] and repair mechanisms [3], and visual processes in the retina [4]. More recently, protein photo-oxidation has been implicated in cataractogenesis [5]. In insects and plants, a flavoprotein named cryptochrome regulates the 24-h circadian clock in a light-dependent fashion [6], whereas at mid-ocean depths, where sunlight scarcely penetrates, most organisms resort to generating their own bioluminescence to distract predators [7] or lure prey [8]. Our understanding of how light energy can be harvested, transduced, and utilized in biological systems is rapidly expanding.

Light can penetrate noninvasively into cells and living tissues, is focused with high spatial and temporal resolution [9–11], and is orthogonal to most biological processes (particularly in mammals). These advantages have led to the study of biological systems using "caged" molecules that are activated with near-UV, visible, or near-IR light [12–16]. For example,

*Corresponding author; ivandmo@sas.upenn.edu; Fax: (215) 573-2122.

Lima et al. microinjected 1-(4,5-dimethoxy-2-nitrophenyl)ethyl (DMNPE)-caged ATP into the central nervous system of *Drosophila* fruit flies to study the role of dopaminergic neurons in the control of movement [13]. Additionally, a caged α-amino-3-hydroxy-5-methyl-4-isoxazolepropionic acid (AMPA) receptor antagonist was developed to monitor surface-exposed AMPA receptors in individual *Xenopus* frog oocytes [14] and in single cells in rat hippocampal cultures [15]. Optogenetics approaches, by which light can trigger the activity of photoresponsive ion channels in individual neurons, powerfully combine genetic targeting of neurons with imaging optics, resulting in photochemical control of cells within intact, living organisms [17–19].

Due to numerous biological processes that are controlled at the genetic level, light-activated oligonucleotides for manipulating DNA, RNA, or protein function hold considerable promise. However, the large size and complexity of oligonucleotides pose challenges in the design and synthesis of caged structures.

Plasmids present special caging challenges as they are too large to synthesize *de novo*. The first caged GFP plasmid was developed by Monroe et al. by reacting DMNPE groups at roughly 270 sites along the phosphate backbone (Fig. 1A) [20]. This construct was intended to block DNA transcription in HeLa cells but its activity could not be fully restored post-photolysis, likely due to the high dose of light needed to remove the large number of caging moieties. Ando et al. advanced this strategy by instead reacting the phosphate backbone of GFP plasmid or GFP mRNA with more photosensitive 6-bromo-4-diazomethyl-7-hydroxycoumarin moieties. This afforded temporal and spatial control over GFP expression in zebrafish embryos upon near-UV irradiation using only one caging group per ~35 bases [21, 22]. Hemphill et al., seeking to circumvent the problems of “statistical caging,” further reduced the number of requisite caging groups by targeting the plasmid promoter region. In this site-specific approach, variations of a promoter sequence with up to three NPOM-caged thymidines were ligated into a GFP reporter plasmid, thereby blocking expression in model mammalian cells and zebrafish embryos until brief (5-minute) 365-nm irradiation [23].

Various caging strategies have also been employed for short oligonucleotides. Pioneering work by Ordoukhanian and Taylor led to the development of a nitrobenzyl-containing phosphoramidite that could be incorporated into a short oligonucleotide strand’s backbone during automated solid-phase synthesis [24]. This resulted in a site-specific strand break upon exposure to 355 nm light, allowing for light-dependent control of oligonucleotide hybridization. Alternate designs for caging small antisense oligonucleotides have involved randomly caging the phosphate backbone (Fig. 1B), e.g., with DMNPE [25] or an iodoacetamide derivative of azobenzene [26]. One improvement was the modification of individual nucleotides (Fig. 1C), such as caged thymidine phosphoramidites, which were incorporated into an oligonucleotide strand during solid-phase synthesis [27, 28]. Phosphorodiamidate morpholino oligomers (MOs) were caged by the Deiters lab with 6-nitropiperonyloxymethyl (NPOM) modified nucleobases to control EGFP expression in cell culture and zebrafish embryos [29]. More recently, the Deiters lab photoregulated miRNA activity in cells by synthesizing reverse complementary oligonucleotides (known as antagomirs) incorporating three or four NPOM-caged bases [30]. This design efficiently

blocked antagomir activity until removal of the caging groups with near-UV light restored native antagomir activity.

Many caging efforts have focused on small interfering RNA (siRNA), which is comprised of short (21–23 base-pair) RNA duplexes that are involved in normal cellular gene regulation but can also be supplied to the cell exogenously. siRNA binds to the RNA-induced silencing complex (RISC), which removes the sense strand, aids in hybridization of the target mRNA to the antisense strand, and finally degrades its mRNA target. Much like other caged oligonucleotides, the earliest examples of photoregulating siRNA involved modifying the phosphate backbone of the siRNA duplex [31, 32]. Another approach has been to incorporate a single caging group (e.g., DMNPE) at the 5′ terminal phosphate of the antisense strand (Fig. 1D) [33] because this phosphate has been shown to be necessary for binding to the RISC complex [34]. Subsequent works by the Friedman group utilized dsRNA precursor duplexes synthesized with both 3′ and 5′ phosphates, which were reacted with diazo-DMNPE to yield more rigorously caged tetra-DMNPE products [35–38]. Finally, caged nucleobases have also been synthesized and incorporated into the antisense strand of siRNA duplexes to photomodulate activity (Fig. 1E) [39].

Recently, caged circular oligonucleotides were designed that remained inactive until photolysis restored target binding (Fig. 1F), aided in part by advances in photocleavable protecting groups [40], novel photolabile phosphoramidites, and controlled porous glasses for functionalizing oligonucleotides during synthesis [41]. Several different circularization strategies have emerged for efficiently caging and uncaging antisense oligonucleotides for applications in developmental biology. In one pioneering example, Tang et al. reported a circular antisense oligonucleotide synthesized as a linear oligonucleotide with 3′-amine and photocleavable linker, 1-(2-nitrophenyl)-1,2-ethanediol, at the 5′-end [42]. The amine and acid groups were joined via a 1-ethyl-3-(3-dimethylaminopropyl) carbodiimide linker. The Chen and Tang labs extended the circular oligonucleotide concept to antisense morpholinos [43, 44]. The Chen lab developed a caged morpholino for the *no tail-a* (*ntla*) gene to study the timing of exocrine fate commitment in zebrafish embryos [43]. Additional work by the Tang lab employed a heterobifunctional photocleavable linker to join the 3′-amine and 5′-carboxylic acid ends of linear morpholinos targeting *beta-catenin-2* and *ntla*, and both genes were successfully photomodulated in zebrafish embryos [44]. More recently, the Tang lab linked two linear oligonucleotides with a photocleavable linker during solid-phase synthesis, and then circularized the oligonucleotide by amide bond formation [45]. They demonstrated that photoactivation of these circular oligonucleotides could turn off GFP expression in cells. These studies confirmed that the circularized, sterically constrained MO is held mostly inactive until disruption of the photolinker reveals the active, linear form.

In these circular caged MO examples, photoactivation was limited to near-UV excitation based on the organic chromophores employed. Expanding photoactivation wavelengths into the visible will reduce phototoxicity, increase depth penetration of the excitation source, and allow for the application of multiple, orthogonally-caged constructs that can be simultaneously delivered and then sequentially photoactivated with high spatiotemporal resolution. The Deiters and Chen labs recently advanced this idea by developing a caged MO using a red-shifted coumarin derivative, [7-(diethylamino)coumarin-4-yl]-methyl

(DEACM), which is responsive to 470 nm light [46]. The DEACM linker was reacted with 5′-amine, 3′-disulfide functionalized MOs in order to cyclize them. By co-injecting zebrafish embryos with 470-nm responsive DEACM-caged *flh* cMO and 365-nm responsive 2-nitrobenzyl-caged *spt* cMO, discrete spatio-temporal control was retained over each gene. Sequential silencing of *flh* followed by *spt* allowed the Deiters and Chen labs to examine the interdependent roles of both genes in axial muscle development in a manner that would have been impossible to achieve with UV-active caging groups alone [46].

It is in this context that we review our lab's efforts for the past decade to develop caged oligonucleotides for controlling gene expression and describe how these caging strategies have been applied by researchers in the field of developmental biology. We highlight a novel visible light-activated ruthenium photolinker, which shows considerable promise for modulating oligonucleotide structure and function in living organisms. Finally, we explain how caged oligonucleotides developed in our laboratory provide the first noninvasive method for harvesting mRNA from single neurons in living brain tissue. We present this work with considerable enthusiasm as photochemistry and imaging methods for studying biological systems, including the brain, are growing rapidly in utility and sophistication (Fig. 2).

2a. Turning gene function "on" using RNA bandages with one photocleavable linker

As tools for turning "on" gene expression, our lab developed RNA bandages, comprised of two antisense oligonucleotides joined by a single photocleavable linker (Fig. 3A) [47]. Each strand was 6–12 nucleotides long and employed 2′-OMe RNA to improve nuclease resistance and mRNA hybridization. The bandages were designed to bind their mRNA target at the start codon and Kozak sequence in the 5′-UTR to block translation until irradiation separated the two strands. In this design, the melting temperatures of the tandem oligonucleotides were significantly lowered after photolysis when compared to the intact RNA bandage. This decreased affinity for the mRNA target allowed the ribosome to bind and translate the mRNA. The best RNA bandage had an "a" strand of 6 nucleotides, "b" strand of 12 nucleotides, a 4-base gap between the strands, and resulted in a 3-fold increase in GFP expression in rabbit reticulocyte lysate after photolysis. However, the bandages required a good deal of optimization, and the bandages with the largest changes in melting temperature were not necessarily the most effective in regulating gene expression [47].

2b. Turning gene function "off" using DNA hairpins with a photocleavable linker

Our lab has also developed tools for turning gene expression "off" with light, in particular caged antisense 18-to-25-mer oligonucleotides that hybridize to an mRNA transcript and either sterically block ribosomal translation or recruit RNaseH to achieve RNA degradation. Caged DNA hairpins are typically comprised of an antisense DNA strand linked via a single photocleavable linker to a complementary blocking strand (Fig. 3B). Through covalent attachment of the antisense and blocking strands, high effective molarity is achieved, and the resulting hairpin possesses high thermal stability prior to photolysis. After irradiation, the strands are no longer linked, which results in much lower melting temperature (T_m): ΔT_m of −30 °C to − 40 °C can be routinely achieved. This promotes strand dissociation and frees the antisense oligonucleotide to bind to its target mRNA. To achieve this initially, a

heterobifunctional linker with maleimide and NHS ester functionalities was created, which allowed reaction with antisense and blocking strands with amine and thiol end-modifications [48]. More recently, we refined this approach by incorporating one or more commercially available phosphoramidite-containing photocleavable linker(s) via solid-phase synthesis [49–52], which has facilitated the synthesis and purification of caged oligonucleotides in much larger quantities.

Our initial *in vivo* studies involved the development of hairpins comprised of negatively charged peptide nucleic acid (PNA) rather than DNA, due to its increased nuclease resistance. These hairpins were successful in photoregulating genes in zebrafish embryos, namely *bozozok* and *chordin* [53]. Our lab subsequently applied DNA hairpins to regulate RNase H-mediated mRNA digestion in cancer cells [54]. These hairpins were phosphorothioated to increase cell stability, and a variety of different blocking strands were tested, through modification of either the 3′ or 5′ end of the antisense oligonucleotide. The Chen lab has optimized the hairpin design for caged antisense morpholino oligonucleotides [55, 56] and applied these caged MOs to gain insight into how *ntla* regulates notochord development in zebrafish [57].

We and others have sought to develop caged oligonucleotides for studying miRNA activity, based on the important roles played by miRNA as negative regulators of target mRNA expression, and the many human diseases that are attributable to miRNA dysregulation. Notably, traditional loss-of-function miRNA studies are not useful for spatially and temporally resolving multiple miRNA functions [58]. While photoregulation of siRNA has been studied for several years [31], miRNA photomodulation has only recently been explored through the development of caged antagomirs, which are complementary to their target miRNA and block miRNA function by outcompeting the target mRNA [59].

The Li lab developed the first caged antagomir, which was a caged hairpin comprised of a 2′-OMe RNA antisense strand for inhibiting a miRNA of interest, linked to a blocking strand via a photoactive, bifunctional linker [60]. While the antagomir was successful at blocking the function of its miRNA target, a small amount of background activity was observed before photolysis because the antisense strand was not completely blocked. One challenge with the single-photocleavable linker caged hairpin design is correlating the pre- and post-photolysis melting temperatures with *in vivo* activity. Biological activity can be tuned by varying the length and placement of the blocking strand, but this optimization process is time-consuming. We recently improved the caging and uncaging efficiency of oligonucleotide hairpins by incorporating a second photocleavable linker [51].

2c. Modulating caging of oligonucleotide hairpins by incorporating two photocleavable linkers

Our lab developed a caged antagomir to photomodulate *let-7* miRNA activity in zebrafish embryos by using a novel caged hairpin design [51]. A 2′-OMe strand antisense to the *let-7* miRNA sequence was caged using two photocleavable groups to divide the blocking strand into two parts (Fig. 3C). This made it possible to lengthen the blocking strand to reduce problems with background activity observed with the Zheng design [60], while maintaining release of the antagomir post-photolysis. As intended, antagomir activity was fully blocked

pre-photolysis and was restored after near-UV irradiation. A very similar caged hairpin with two photocleavable linkers has proven to be remarkably useful for harvesting mRNA from living cells (Fig. 3D), as described later.

2d. Turning gene function "off" using caged circular oligonucleotides

To engineer the first example of a caged miRNA, our lab employed a 2-photocleavable linker circular design strategy (Fig. 3E) [51], which we had originally employed for caging DNAzymes [49]. A circular caged *let-7* miRNA comprised of a 22-mer 2′-OMe miRNA, blocking strand, and two photocleavable spacers was synthesized with a free 3′ amine and 5′ thiol, and these ends were joined with a commercially available heterobifunctional linker [51]. As with previous circular oligonucleotide designs [42-45, 49], no background activity was observed in zebrafish embryos before photolysis, but the activity of the exogenous miRNA was restored post-photolysis. The versatility of employing two photocleavable linkers to turn *let-7* miRNA "on" or "off" with light is highlighted in Fig. 4.

2e. New ruthenium photolinkers for caging oligonucleotides

To improve capabilities for multiplexed caging/uncaging experiments involving visible-light or 2-photon (near-IR) excitation, our laboratory has recently developed a synthetically versatile class of bis(bipyridine)ruthenium(II) photolinkers. $[Ru(bpy)_2L_2]^{2+}$ complexes are well known to undergo facile ligand (L) exchange with solvent upon 400-500 nm (1-photon) or 800–1,000 nm (2-photon) excitation, making this an attractive inorganic caging moiety [61]. Etchenique and co-workers have developed a variety of bioactive, pyridine- or amine-bearing ligands that can be released from $[Ru(bpy)_2L_2]^{2+}$ with visible light [62, 63], and concurrent work by the Turro Lab has focused on Ru-based photodynamic therapeutics [64–66]. The Etchenique and Yuste labs have since collaborated on ruthenium-caged glutamate and dopamine compounds, which can be released in single cells of living brain slices using 2-photon near-infrared excitation without any apparent toxicity [67, 68]. Building on this foundation, our lab recently developed the first ruthenium photolinker, $Ru^{2+}(bpy)_2$(bis(3-ethynylpyridine)) (RuBEP) [69]. The two photolabile ligands of RuBEP present alkynes that can react with 3′ and 5′ terminal azides of an oligonucleotide in Cu(I)-catalyzed azide-alkyne cycloaddition (CuAAC) reactions to yield a circular, caged construct (Fig. 5). To validate this new photolinker we synthesized Ru-caged MOs targeting the zebrafish genes *chordin* or *notail*: when zebrafish microinjected with the Ru-caged MO were irradiated with 450 nm light, one of RuBEP's pyridyltriazole ligands was exchanged with water ($\Phi = 0.33$ in ambient conditions), and the biologically active MO was able to knockdown gene expression [69]. The promising results observed with the first Ru-caged MOs and the versatile photochemistry of ruthenium polypyridyl complexes motivate our development of new ruthenium photolinkers. For example, ruthenium photolinkers absorbing at different visible wavelengths will expand multiplexing capabilities and address the lingering necessity for UV-irradiation found in the previously discussed DEACM + NB methods [46].

3. Transcriptome *In Vivo* Analysis (TIVA)

In many areas of biology, there is a growing desire to probe the RNA complement—the transcriptome—in individual cells within intact living tissue. Differing amounts of specific

RNAs to a large extent determine cell morphology and function [70]. The requirement to perform experiments in single cells arises from the fact that there are many cell types and there is significant mRNA heterogeneity even from cells of similar origin. In neurobiology, most approaches for isolating mRNA from neurons do not work in complex brain tissue, and the ones that do (e.g., patch pipette [71, 72] and AFM nanoprobe methods [73]) involve risk of contamination and mechanical injury to the cells. Our laboratory, with UPenn collaborator James Eberwine, has sought to develop a noninvasive method for capturing mRNA from single neurons in live brain slices. We describe here a prototypal Transcriptome *In Vivo* Analysis (TIVA) caged oligonucleotide construct. TIVA-isolated mRNA can be subsequently amplified and analyzed by next-generation RNA sequencing (RNA-seq) [52].

In developing TIVA, we built on the success of our previous caged oligonucleotide designs employing two photocleavable linkers. The resulting TIVA construct (Fig. 6A) is a highly derivatized caged hairpin, conceptually similar to the aforementioned caged antagomir (Fig. 3C). The antisense strand is linked via a photocleavable spacer to a bipartite, photoactive blocking strand. Upon photolysis, the blocking strand is broken into two shorter oligonucleotides, which can dissociate from the antisense strand more easily, as indicated by ΔT_m of −35 °C. This allows the blocking strands to cover the entire antisense strand, efficiently blocking it from binding to its target mRNA. This eliminates problems with pre-photolysis background activity. Because mRNAs have a 3′-polyadenine tail that aids in translation, our TIVA probe strand consists of uracils that can hybridize to this region of mRNA. This portion of the oligonucleotide is comprised of 2′-fluoro RNA, which is an RNA analog with increased thermal stability and nuclease resistance. The two photocleavable spacers are incorporated to join the 2′-fluoro-U probe strand to the two shorter 2′-OMe RNA poly(A) blocking strands. A 3′-biotin tag was added to allow for isolation with streptavidin beads, and a cell-penetrating peptide (CPP) consisting of nine arginine residues was incorporated to promote cellular uptake. Finally, Cy3 and Cy5 fluorophores were introduced as a fluorescence resonance energy transfer (FRET) pair. One experimental paradigm with TIVA is highlighted in Fig. 6B: Fluorescence imaging of live brain tissue was performed to confirm cell uptake, followed by selective 405-nm laser activation in single neurons. Gain of Cy3 emission and loss of Cy5 emission (indicating loss of FRET signal) confirmed that dissociation of the TIVA oligonucleotide (allowing mRNA capture) occurred after photolysis.

TIVA provides a minimally invasive method for harvesting mRNA from single cells in living brain tissue, which has made it possible to study the role of the neuronal microenvironment in controlling transcriptional variability [52]. TIVA has the potential to impact our understanding of transcriptomics in many areas of neurobiology, such as aging, learning and memory, as well as in developmental biology, human disease, and drug discovery. Moving TIVA studies from live tissue slices to whole organisms has shown initial promise, though several challenges remain. Caging stability must be fortified, potentially through the use of longer hairpins, unnatural backbones, or protective carrier compounds. While $(Arg)_9$ provides good cytosolic delivery into a variety of common cell types, it can be easily swapped out with other CPP sequences to optimize probe uptake and

internal trafficking in cells with poor $(Arg)_9$ compatibility. To enable both deeper tissue penetration and multiplexing capabilities, we are now applying Ru-caging strategies to TIVA. TIVA constructs employing a ruthenium photolinker rather than nitrobenzyl photocleavable linkers will overcome current disadvantages associated with near-UV irradiation, effectively expanding the utility of the TIVA approach.

4. Conclusions and future directions

Recent events highlight the role for oligonucleotides as a new and rapidly developing class of therapeutic agents. In 2013, the FDA approved the second RNA-based drug, mipomersen, which is a 2′-O-methoxyethyl phosphorothioate antisense oligonucleotide targeting apolipoprotein B expressed in the liver [74]. By reducing the amount of this protein that is secreted from the liver into the blood stream, mipomersen successfully decreases low-density lipoprotein cholesterol levels in patients with homozygous familial hypercholesterolemia [75]. RNA therapeutics have also captured the public's attention in the fight against Ebola and other deadly viruses. And, clinical trials are being conducted with siRNA for the treatment of macular degeneration, an antisense RNA molecule targeting an anti-apoptotic chaperone protein upregulated in cancer cells, and a splice-switching oligonucleotide for treating Duchenne muscular dystrophy [76]. These latest advances underscore the challenges, but also huge potential, for oligonucleotide therapeutics in humans. It is worth considering whether caging strategies highlighted in this review could improve cell targeting, and thereby reduce immune response and systemic toxicity.

Our lab's recent examples of a caged antagomir, caged circular miRNA, and TIVA illustrate how the use of two photocleavable linkers can streamline the design process and improve photomodulation characteristics, with little decrement in photo-uncaging efficiency. One remaining challenge is to uncage oligonucleotides at greater depths in biological samples and living organisms. Caging moieties that exhibit higher extinction coefficients at longer (visible) wavelengths can expand biological applications [29, 77–79]. Moreover, a few groups have succeeded in caging oligonucleotides with two-photon-activatable moieties that should allow greater penetration of tissue with light and improved depth discrimination [79–81]. Ruthenium photolinkers being developed in our laboratory are also a significant step in this direction due to the versatile one- and two-photon photochemistry of $[Ru(bpy)_2(L)_2]^{2+}$ complexes [69]. Ruthenium photolinkers provide a compact, rigid structural motif that is useful for enforcing caged conformations. Finally, Ru-polypyridyl chemistry offers tremendous synthetic flexibility, which will soon provide unique multiplexing capabilities for selective Ru-oligonucleotide uncaging at high spatial and temporal resolution.

Acknowledgments

We thank Drs. XinJing Tang, Julia Richards, and Julianne Griepenburg for their many contributions to the development of light-activated oligonucleotides in our laboratory, as highlighted in this review. For the TIVA project, we acknowledge Dr. James Eberwine and coworkers for a productive collaboration, with particular thanks to Drs. Jaehee Lee and Jai-Yoon Sul for generating Figure 6B. This work was supported by NIH R-01 GM083030, a Camille and Henry Dreyfus Teacher-Scholar Award, and a McKnight Technological Innovations in Neuroscience Award.

Abbreviations

AMPA	α-amino-3-hydroxy-5-methyl-4-isoxazolepropionic acid
CuAAC	Cu(I)-catalyzed alkyne + azide cycloaddition
DEACM	[7-(diethylamino)coumarin-4-yl]-methyl
DMNPE	1-(4,5-dimethoxy-2-nitrophenyl)ethyl
FRET	fluorescence resonance energy transfer
MOs	Morpholino oligonucleotides
NPOM	6-nitropiperonyloxymethyl
RNAi	RNA interference
siRNA	small interfering RNA
TIVA	Transcriptome *In Vivo* Analysis

References

1. Jensen RG, Bassham JA. Proc Natl Acad Sci U S A. 1966; 56:1095–1101. [PubMed: 5339288]
2. Pattison DI, Davies MJ EXS. 2006:131–157.
3. Biernat MA, Eker AP, van Oers MM, Vlak JM, van der Horst GT, Chaves I. J Biol Rhythms. 2012; 27:3–11. [PubMed: 22306969]
4. Palczewski K, Kumasaka T, Hori T, Behnke CA, Motoshima H, Fox BA, Le Trong I, Teller DC, Okada T, Stenkamp RE, Yamamoto M, Miyano M. Science. 2000; 289:739–745. [PubMed: 10926528]
5. Davies MJ, Truscott RJ. J Photochem Photobiol B. 2001; 63:114–125. [PubMed: 11684458]
6. Partch CL, Shields KF, Thompson CL, Selby CP, Sancar A. Proc Natl Acad Sci U S A. 2006; 103:10467–10472. [PubMed: 16790549]
7. Haddock SHD, Case JF. Nature. 1994; 367:225–226.
8. Haddock SHD, Dunn CW, Pugh PR, Schnitzler CE. Science. 2005; 309:263. [PubMed: 16002609]
9. Burgalossi A, Jung S, Man KN, Nair R, Jockusch WJ, Wojcik SM, Brose N, Rhee JS. Nat Protoc. 2012; 7:1351–1365. [PubMed: 22722370]
10. Shroff H, Galbraith CG, Galbraith JA, Betzig E. Nat Meth. 2008; 5:417–423.
11. Hess ST, Girirajan TP, Mason MD. Biophys J. 2006; 91:4258–4272. [PubMed: 16980368]
12. Gardner L, Zou Y, Mara A, Cropp TA, Deiters A. Mol Biosyst. 2011; 7:2554–2557. [PubMed: 21785768]
13. Lima SQ, Miesenbock G. Cell. 2005; 121:141–152. [PubMed: 15820685]
14. Chambers JJ, Gouda H, Young DM, Kuntz ID, England PM. J Am Chem Soc. 2004; 126:13886–13887. [PubMed: 15506725]
15. Adesnik H, Nicoll RA, England PM. Neuron. 2005; 48:977–985. [PubMed: 16364901]
16. Makings LR, Tsien RY. J Biol Chem. 1994; 269:6282–6285. [PubMed: 8119976]
17. Deisseroth K, Feng G, Majewska AK, Miesenbock G, Ting A, Schnitzer MJ. J Neurosci. 2006; 26:10380–10386. [PubMed: 17035522]
18. Fehrentz T, Schonberger M, Trauner D. Angew Chem Int Ed. 2011; 50:12156–12182.
19. Muller K, Weber W. Mol Biosyst. 2013; 9:596–608. [PubMed: 23412367]
20. Monroe WT, McQuain MM, Chang MS, Alexander JS, Haselton FR. J Biol Chem. 1999; 274:20895–20900. [PubMed: 10409633]
21. Ando H, Furuta T, Tsien RY, Okamoto H. Nat Genet. 2001; 28:317–325. [PubMed: 11479592]

22. Ando H, Kobayashi M, Tsubokawa T, Uyemura K, Furuta T, Okamoto H. Dev Biol. 2005; 287:456–468. [PubMed: 16226737]
23. Hemphill J, Govan J, Uprety R, Tsang M, Deiters A. J Am Chem Soc. 2014; 136:7152–7158. [PubMed: 24802207]
24. Ordoukhanian P, Taylor JS. J Am Chem Soc. 1995; 117:9570–9571.
25. Ghosn B, Haselton FR, Gee KR, Monroe WT. Photochem Photobiol. 2005; 81:953–959. [PubMed: 15869326]
26. Patnaik S, Kumar P, Garg BS, Gandhi RP, Gupta KC. Bioorg Med Chem. 2007; 15:7840–7849. [PubMed: 17870546]
27. Krock L, Heckel A. Angew Chem Int Ed. 2005; 44:471–473.
28. Young DD, Lusic H, Lively MO, Yoder JA, Deiters A. Chembiochem. 2008; 9:2937–2940. [PubMed: 19021142]
29. Deiters A, Garner RA, Lusic H, Govan JM, Dush M, Nascone-Yoder NM, Yoder JA. J Am Chem Soc. 2010; 132:15644–15650. [PubMed: 20961123]
30. Connelly CM, Uprety R, Hemphill J, Deiters A. Mol Biosyst. 2012; 8:2987–2993. [PubMed: 22945263]
31. Shah S, Rangarajan S, Friedman SH. Angew Chem Int Ed. 2005; 44:1328–1332.
32. Blidner RA, Svoboda KR, Hammer RP, Monroe WT. Mol Biosyst. 2008; 4:431–440. [PubMed: 18414741]
33. Nguyen QN, Chavli RV, Marques JT, Conrad PG Jr, Wang D, He W, Belisle BE, Zhang A, Pastor LM, Witney FR, Morris M, Heitz F, Divita G, Williams BR, McMaster GK. Biochim Biophys Acta. 2006; 1758:394–403. [PubMed: 16497269]
34. Martinez J, Patkaniowska A, Urlaub H, Luhrmann R, Tuschl T. Cell. 2002; 110:563–574. [PubMed: 12230974]
35. Shah S, Jain PK, Kala A, Karunakaran D, Friedman SH. Nucleic Acids Res. 2009; 37:4508–4517. [PubMed: 19477960]
36. Jain PK, Shah S, Friedman SH. J Am Chem Soc. 2011; 133:440–446. [PubMed: 21162570]
37. Kala A, Jain PK, Friedman SH. Mol Biosyst. 2014; 10:1689–1692. [PubMed: 24531692]
38. Kala A, Jain PK, Karunakaran D, Shah S, Friedman SH. Nat Protoc. 2014; 9:11–20. [PubMed: 24309973]
39. Mikat V, Heckel A. RNA. 2007; 13:2341–2347. [PubMed: 17951332]
40. Coleman MP, Boyd MK. J Org Chem. 2002; 67:7641–7648. [PubMed: 12398484]
41. Su M, Wang J, Tang X. Chemistry. 2012; 18:9628–9637. [PubMed: 22767502]
42. Tang X, Su M, Yu L, Lv C, Wang J, Li Z. Nucleic Acids Res. 2010; 38:3848–3855. [PubMed: 20164090]
43. Yamazoe S, Shestopalov IA, Provost E, Leach SD, Chen JK. Angew Chem Int Ed. 2012; 51:6908–6911.
44. Wang Y, Wu L, Wang P, Lv C, Yang Z, Tang X. Nucleic Acids Res. 2012; 40:11155–11162. [PubMed: 23002141]
45. Wu L, Wang Y, Wu J, Lv C, Wang J, Tang X. Nucleic Acids Res. 2013; 41:677–686. [PubMed: 23104375]
46. Yamazoe S, Liu Q, McQuade LE, Deiters A, Chen JK. Angew Chem Int Ed. 2014; 53:10114–10118.
47. Richards JL, Tang X, Turetsky A, Dmochowski IJ. Bioorg Med Chem Lett. 2008; 18:6255–6258. [PubMed: 18926697]
48. Tang X, Dmochowski IJ. Angew Chem Int Ed. 2006; 45:3523–3526.
49. Richards JL, Seward GK, Wang YH, Dmochowski IJ. Chembiochem. 2010; 11:320–324. [PubMed: 20077457]
50. Ruble BK, Richards JL, Cheung-Lau JC, Dmochowski IJ. Inorg Chim Acta. 2012; 380:386–391.
51. Griepenburg JC, Ruble BK, Dmochowski IJ. Bioorg Med Chem. 2013; 21:6198–6204. [PubMed: 23721917]

52. Lovatt D, Ruble BK, Lee J, Dueck H, Kim TK, Fisher S, Francis C, Spaethling JM, Wolf JA, Grady MS, Ulyanova AV, Yeldell SB, Griepenburg JC, Buckley PT, Kim J, Sul JY, Dmochowski IJ, Eberwine J. Nat Meth. 2014; 11:190–196.
53. Tang X, Maegawa S, Weinberg ES, Dmochowski IJ. J Am Chem Soc. 2007; 129:11000–11001. [PubMed: 17711280]
54. Tang X, Swaminathan J, Gewirtz AM, Dmochowski IJ. Nucleic Acids Res. 2008; 36:559–569. [PubMed: 18056083]
55. Ouyang X, Shestopalov IA, Sinha S, Zheng G, Pitt CL, Li WH, Olson AJ, Chen JK. J Am Chem Soc. 2009; 131:13255–13269. [PubMed: 19708646]
56. Shestopalov IA, Sinha S, Chen JK. Nat Chem Biol. 2007; 3:650–651. [PubMed: 17717538]
57. Shestopalov IA, Pitt CL, Chen JK. Nat Chem Biol. 2012; 8:270–276. [PubMed: 22286130]
58. Stenvang J, Petri A, Lindow M, Obad S, Kauppinen S. Silence. 2012; 3:1. [PubMed: 22230293]
59. Krutzfeldt J, Rajewsky N, Braich R, Rajeev KG, Tuschl T, Manoharan M, Stoffel M. Nature. 2005; 438:685–689. [PubMed: 16258535]
60. Li WH, Zheng G. Photochem Photobiol Sci. 2012; 11:460–471. [PubMed: 22252510]
61. Zayat L, Filevich O, Baraldo LM, Etchenique R. Philos Trans A Math Phys Eng Sci. 2013; 371:20120330. [PubMed: 23776299]
62. Zayat L, Calero C, Albores P, Baraldo L, Etchenique R. J Am Chem Soc. 2003; 125:882–883. [PubMed: 12537482]
63. Zayat L, Salierno M, Etchenique R. Inorg Chem. 2006; 45:1728–1731. [PubMed: 16471986]
64. Singh TN, Turro C. Inorg Chem. 2004; 43:7260–7262. [PubMed: 15530069]
65. Garner RN, Gallucci JC, Dunbar KR, Turro C. Inorg Chem. 2011; 50:9213–9215. [PubMed: 21879748]
66. Sears RB, Joyce LE, Ojaimi M, Gallucci JC, Thummel RP, Turro C. J Inorg Biochem. 2013; 121:77–87. [PubMed: 23353083]
67. Araya R, Andino-Pavlovsky V, Yuste R, Etchenique R. ACS Chem Neurosci. 2013; 4:1163–1167. [PubMed: 23672485]
68. Fino E, Araya R, Peterka DS, Salierno M, Etchenique R, Yuste R. Frontiers Neural Circuits. 2009; 310.3389/neuro.3304.3002.2009
69. Griepenburg JC, Rapp TL, Carroll PJ, Eberwine J, Dmochowski IJ. Chem Sci. 2015
70. Sul JY, Wu CW, Zeng F, Jochems J, Lee MT, Kim TK, Peritz T, Buckley P, Cappelleri DJ, Maronski M, Kim M, Kumar V, Meaney D, Kim J, Eberwine J. Proc Natl Acad Sci U S A. 2009; 106:7624–7629. [PubMed: 19380745]
71. Eberwine J, Yeh H, Miyashiro K, Cao Y, Nair S, Finnell R, Zettel M, Coleman P. Proc Natl Acad Sci U S A. 1992; 89:3010–3014. [PubMed: 1557406]
72. Van Gelder RN, von Zastrow ME, Yool A, Dement WC, Barchas JD, Eberwine JH. Proc Natl Acad Sci U S A. 1990; 87:1663–1667. [PubMed: 1689846]
73. Uehara H, Ikai A, Osada T. Meth Mol Biol. 2009; 544:599–608.
74. Hair P, Cameron F, McKeage K. Drugs. 2013; 73:487–493. [PubMed: 23564617]
75. McGowan MP, Tardif JC, Ceska R, Burgess LJ, Soran H, Gouni-Berthold I, Wagener G, Chasan-Taber S. PLoS One. 2012; 7:e49006. [PubMed: 23152839]
76. Kole R, Krainer AR, Altman S. Nat Rev Drug Discov. 2012; 11:125–140. [PubMed: 22262036]
77. Menge C, Heckel A. Org Lett. 2011; 13:4620–4623. [PubMed: 21834506]
78. Schafer F, Joshi KB, Fichte MA, Mack T, Wachtveitl J, Heckel A. Org Lett. 2011; 13:1450–1453. [PubMed: 21341754]
79. Lusic H, Uprety R, Deiters A. Org Lett. 2010; 12:916–919. [PubMed: 20112966]
80. Furuta T, Watanabe T, Tanabe S, Sakyo J, Matsuba C. Org Lett. 2007; 9:4717–4720. [PubMed: 17929824]
81. Li Y, Shi J, Luo Z, Jiang H, Chen X, Wang F, Wu X, Guo Q. Bioorg Med Chem Lett. 2009; 19:5368–5371. [PubMed: 19682894]

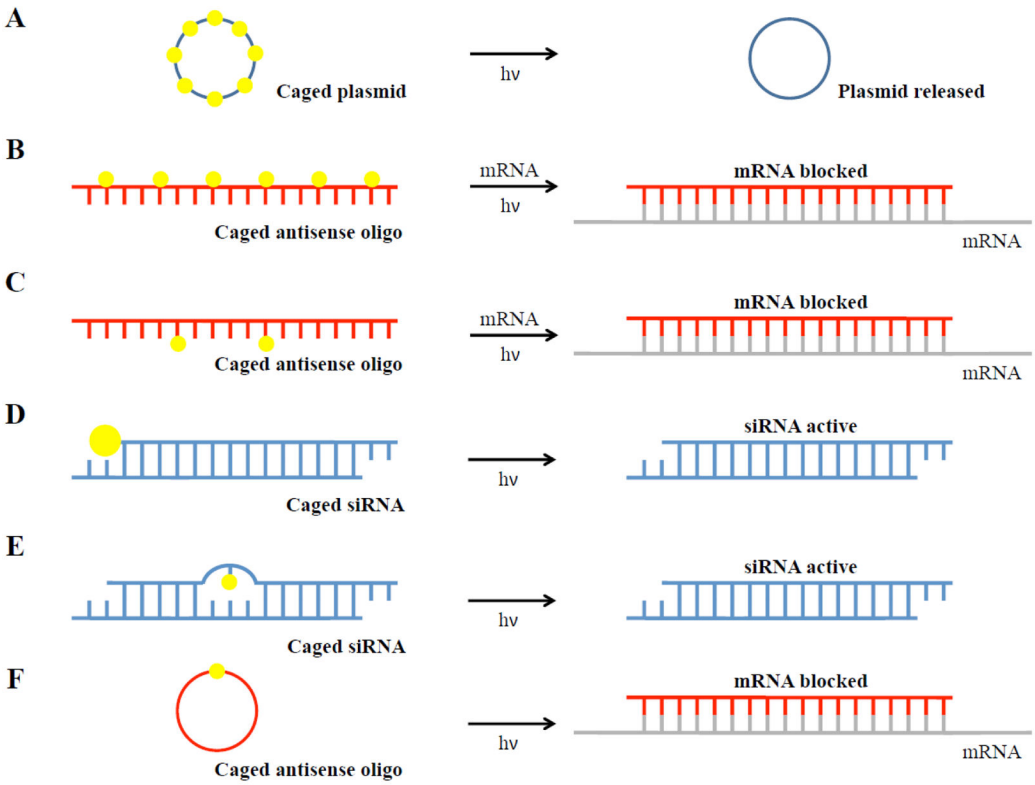

Figure 1.

Various approaches for caging oligonucleotide function using photoresponsive blocking groups or linkers (in yellow). (A) Plasmid with phosphate backbone caged is unable to be expressed until photolysis with near-UV light removes the caging groups. (B) Caging of the phosphate backbone of antisense oligonucleotides prevents them from hybridizing to their mRNA target until the caging groups are removed with light. (C) Antisense oligonucleotides with caged nucleobases incorporated during solid phase synthesis are unable to bind their target. After irradiation with near-UV light, the caging moieties are removed, allowing the antisense strand to bind its target. (D) siRNA molecules caged at the 5′-end of the antisense strand are inactive until after near-UV exposure. (E) When caged bases are incorporated in the center of a siRNA strand, a bulge results, blocking the activity of the siRNA until it is exposed to light. (F) Circular caged oligonucleotides are completely inactive until the molecules are irradiated.

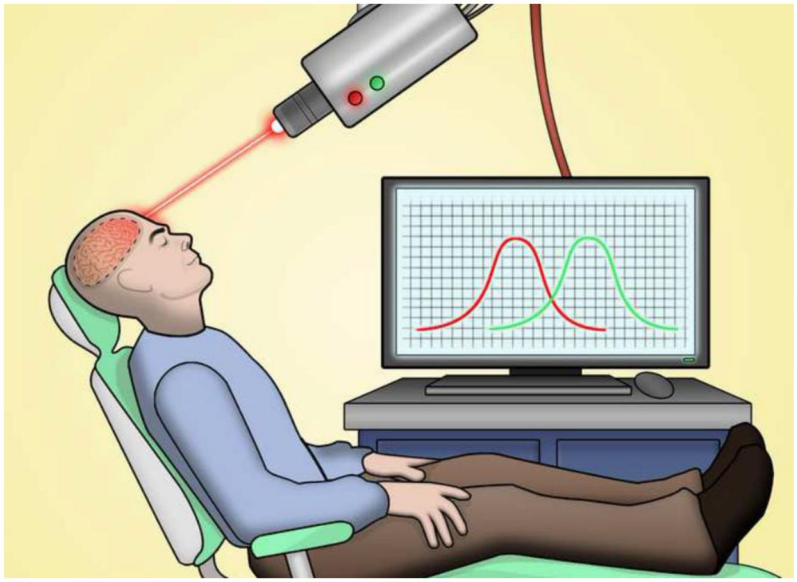

Figure 2.

"We're finally getting somewhere!" New photochemical approaches stoke the imagination for the potential uses of caged oligonucleotides in neuroscience and other biological applications.

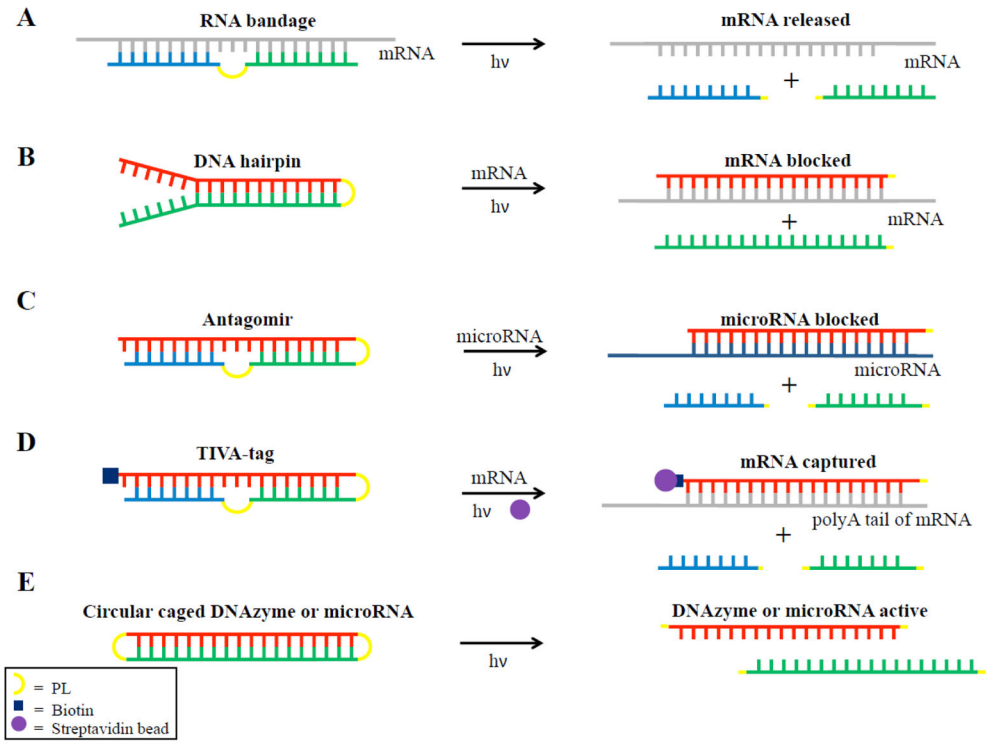

Figure 3.

Caged oligonucleotide strategies developed in the Dmochowski lab. (A) RNA bandages consist of two tandem oligonucleotides (green and blue) linked by a photocleavable linker (yellow). Prior to irradiation, the bandage binds the mRNA target to prevent translation. After photolysis, the short oligonucleotide strands dissociate from the mRNA, allowing translation to occur. (B) DNA hairpins are comprised of an antisense oligonucleotide (red) linked via a photocleavable linker to a blocking strand (green). Upon near-UV irradiation, the antisense strand is able to bind to its mRNA target (gray) and inhibit translation. (C) Antagomirs are structurally similar to hairpins, but the blocking strand (green and blue) is divided into two parts by a second photocleavable linker. This design allows the blocking strand to be as long as possible before uncaging, efficiently blocking the antisense strand from binding to its target microRNA. (D) Transcriptome *In Vivo* Analysis (TIVA) tags are comprised of an antisense strand (red) linked via a photocleavable spacer to a blocking strand (green and blue) that is divided into two parts by a second photocleavable linker. After photolysis, the antisense strand is able to bind the poly-A tail of mRNA. By incorporating a biotin group at the 3′-end of the oligo, streptavidin beads can be added to isolate the mRNA bound to the TIVA tag. (E) DNAzymes and microRNA molecules can be caged by synthesizing oligonucleotides with photocleavable linkers and then circularizing. Exposure to near-UV light results in release of the active, linear oligo.

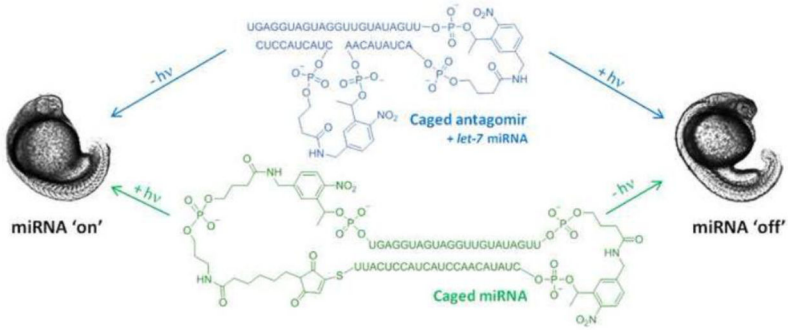

Figure 4.

Strategies for turning microRNA “on” or “off” in developing zebrafish embryos. Caged hairpin antagomir (blue) with two photocleavable nitrobenzyl groups blocked *let-7* miRNA function in zebrafish embryos after photolysis with near-UV light. Circular caged *let-7* miRNA (green) was activated in zebrafish embryos upon irradiation with near-UV light. Adapted from ref 51.

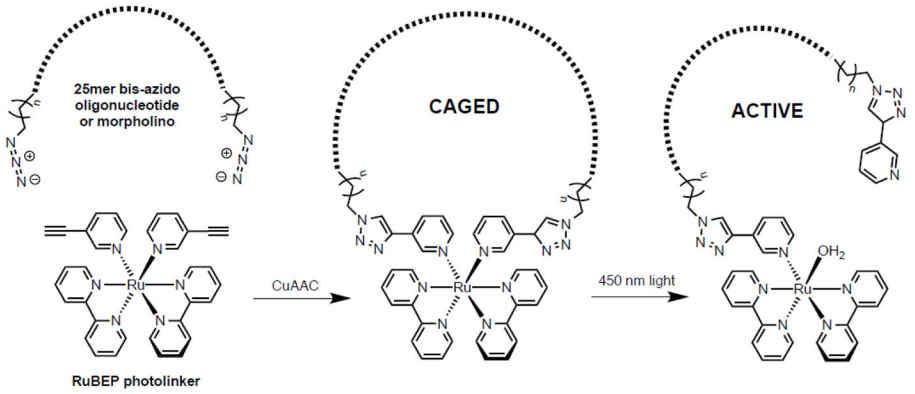

Figure 5.

Bis-azido oligonucleotides reacted with RuBEP photolinker were circularized and remained "caged" until activated with 450 nm light.

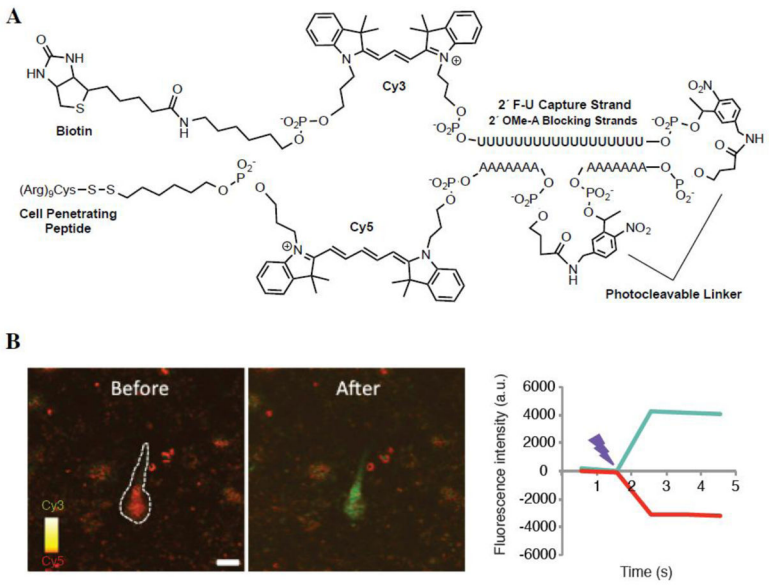

Figure 6.

Transcriptome *In Vivo* Analysis (TIVA) is a powerful tool for single-cell mRNA capture. (A) Structural diagram of TIVA-tag conjugated to an $(Arg)_9$ cell penetrating peptide. (B) Spatially and temporally selective, 405-nm laser activation of TIVA construct in live brain tissue. Photoactivation in one cell soma (delineated by solid white line) produced significant loss of FRET signal, with greater Cy3 donor emission evident in “After” image and graph. Second cell soma (delineated by dashed white line) was not photoactivated, and no change in FRET signal was observed.